
Isotopic time-series partitioning of streamflow components in wetland-dominated catchments, lower Liard River basin, Northwest Territories, Canada

Natalie A. St Amour,^{1*} John J. Gibson,² Thomas W. D. Edwards,¹ Terry D. Prowse² and Alain Pietroniro³

¹ *Department of Earth Sciences, University of Waterloo, Waterloo, ON, Canada*

² *National Water Research Institute, Water & Climate Impacts Research Centre, Victoria, BC, Canada*

³ *National Water Research Institute, Saskatoon, SK, Canada*

Abstract:

The distribution of stable water isotopes provides valuable insight into runoff generation processes in subarctic wetland regions of the Mackenzie River basin, a major freshwater contributor to the Arctic Ocean and the focus of intensive hydrological research as part of Canada's contribution to the Global Energy and Water Cycle Experiment (GEWEX). This article describes a streamflow hydrograph separation analysis carried out over three complete annual cycles (1997–1999) for five subarctic catchments ranging in size from 202 to 2050 km² situated near the confluence of the Liard and Mackenzie rivers. This heterogeneous landscape, characterized by extensive wetlands (fen and bog), shallow lakes and widespread discontinuous permafrost, is representative of vast flow-contributing areas of the upper Mackenzie Valley, and is suspected to be highly sensitive to climate variability and change. We document seasonal patterns and interannual variability in the isotopic composition of local streamflow, attributable to mixing of three distinctly labelled flow sources, namely groundwater, surface water plus rain, and direct snowmelt, and apply these isotopic signals to partition sources and their temporal variability. Although groundwater input is the dominant and most persistent streamflow source in all five catchments throughout the year, direct snowmelt runoff via surface and shallow subsurface pathways (during spring freshet) and surface waters from lakes and wetlands situated in low-lying areas of the basins (during summer and fall) are also significant seasonal contributors. Catchment-specific differences are also apparent, particularly in the generation of snowmelt runoff, which is more attenuated in fen-dominated than in bog-dominated catchments. The data set additionally reveals notable interannual variability in snow isotope signatures and snow water equivalent, apparently enhanced by the 1998 El Niño event. Copyright © 2005 John Wiley & Sons, Ltd.

KEY WORDS oxygen-18; deuterium; hydrograph separation; peatlands; snowmelt; surface waters; *d*-excess; snow water equivalent; discontinuous permafrost

INTRODUCTION

The lowland terrain around the confluence of the Liard and Mackenzie rivers is characterized by extensive subarctic wetlands containing myriad peatlands (fens and bogs), scattered shallow lakes, and the widespread occurrence of discontinuous permafrost (Figure 1). Understanding the hydrology of such wetlands, which extend over large areas of the circumpolar north, is crucial because of their global importance in modulating freshwater fluxes to the Arctic Ocean and their inherent sensitivity to climate variability and change. Indeed, the Mackenzie basin has seen the most pronounced and persistent increase in mean annual temperature within Canada over the past few decades (Stewart *et al.*, 1998; Folland *et al.*, 2001) and associated hydrological changes are undoubtedly occurring (Rouse, 2000). Postulated changes in the hydrological regime include

* Correspondence to: Natalie A. St Amour, Department of Earth Sciences, University of Waterloo, 200 University Ave W, Waterloo, Ontario N2L 3G1, Canada. E-mail: nastamou@scimail.uwaterloo.ca

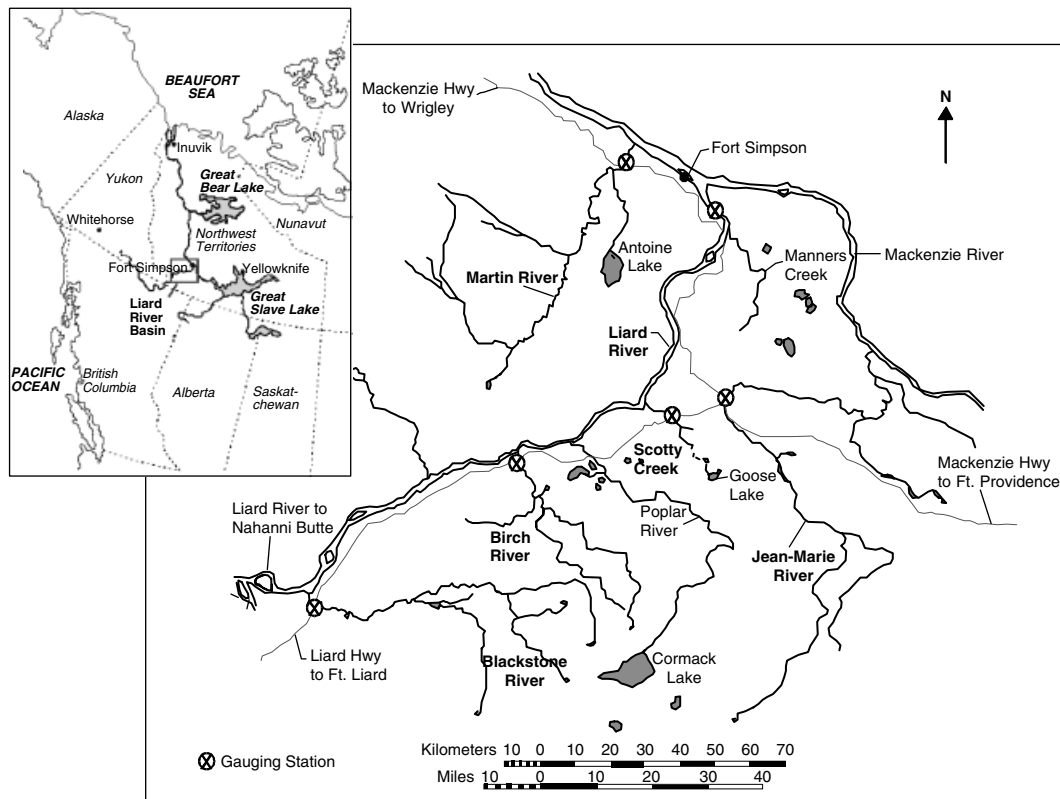


Figure 1. Map of Fort Simpson area, Northwest Territories, Canada, showing location of discharge gauging stations for the rivers studied. Names of other rivers and lakes mentioned in the paper are also included for reference

degradation of permafrost, enhancement of evaporation rates, decline in surface water storage, and deepening or alteration of groundwater flow paths, as well as alteration of the amount, nature and seasonal timing of precipitation. More sophisticated understanding of these runoff controls is required to predict the hydrological consequences of climate change and variability and, in particular, to establish the cumulative impacts and feedbacks between the land surface and atmospheric water cycles and effects on discharge to the Arctic Ocean.

There is a considerable body of knowledge on hydrological processes in subarctic wetland catchments, which provide valuable context for interpreting interbasinal variations in the partitioning of major streamflow sources observed in this study. Important features controlling runoff in the region include: (i) the presence and distribution of fens and bogs, which often establish hydrological routing and storage availability (e.g. Woo and Heron, 1987; Woo and diCenzo, 1989; Woo and Winter, 1993; Quinton and Roulet, 1998; Hayashi *et al.*, 2004); (ii) aspect and vegetation, which identify areas likely to be affected by permafrost (e.g. Gibson *et al.*, 1993b) and significantly control snow distribution and snowmelt response (e.g. Price, 1987; Woo and Heron, 1987; Woo and diCenzo, 1989; Yang and Woo, 1999); and (iii) surficial geology, which exerts an overriding control on the groundwater regime. In general, fens and lakes receive lateral water inputs from surface water and groundwater flow plus precipitation, whereas bogs are sustained by precipitation (Zoltai *et al.*, 1988; National Wetlands Working Group, 1997).

Natural variability in the stable isotopes of water in runoff sources and streamflow has been applied in high-latitude regions to trace evolution of flow contributions to discharge, particularly during the dominant spring melt event (e.g. Obradovic and Sklash, 1986; Rodhe, 1987, 1998; Gibson *et al.*, 1993b; Harris *et al.*, 1995; McNamara *et al.*, 1998; Laudon *et al.*, 2004). Using a similar approach to monitor five nearby watersheds

simultaneously, this study was designed to examine interbasin variability of distinctly labelled runoff sources, including: (1) groundwater, having an isotopic composition similar to local amount-weighted mean annual precipitation; (2) snowpack, having a depleted isotopic signature; one that is liberated and introduced rapidly to the water phase during the spring freshet; and (3) surface water, variably enriched in heavy isotopes due to evaporation and from admixture of rain during the thaw season. As described in detail below, the streamflow partitioning strategy we employ provides considerable insight into the temporal controls on runoff sources and variability in a complex, wetland-dominated area. Through comparison with several key catchment-specific factors, including topographic gradients, land surface cover, and snowpack distribution, we also begin to explain some of the dominant causes of spatial variability in runoff sources across the region.

THEORY

Systematic seasonal isotopic labelling of precipitation is typical at high latitudes (Edwards *et al.*, 2004). During the year, isotopic signals of source waters propagate through catchments via surface and shallow subsurface runoff and merge into streams, to produce an integrated isotopic signal. Prior efforts to characterize the isotopic composition of streamflow and the identification of its primary source waters in wetlands within the lower Liard basin (Gibson *et al.*, 1993a,b; Reedyk *et al.*, 1995; Gibson and Prowse, 1999, 2002) have established a strong understanding of seasonal variability in the streamflow signal, as illustrated in Figure 2 and conceptually in Figure 3a. Hence, the isotopic composition of streamflow can be considered to cycle annually among variably well-defined 'set-points' in $\delta^2\text{H}$ – $\delta^{18}\text{O}$ space (shaded ovals, Figure 3a; also see Gibson and Prowse (2002)). Streamflow during late summer and fall tends to contain the highest proportion of surface water derived from wetlands and lakes, as well as rain, and, therefore, attains an isotopically enriched signature

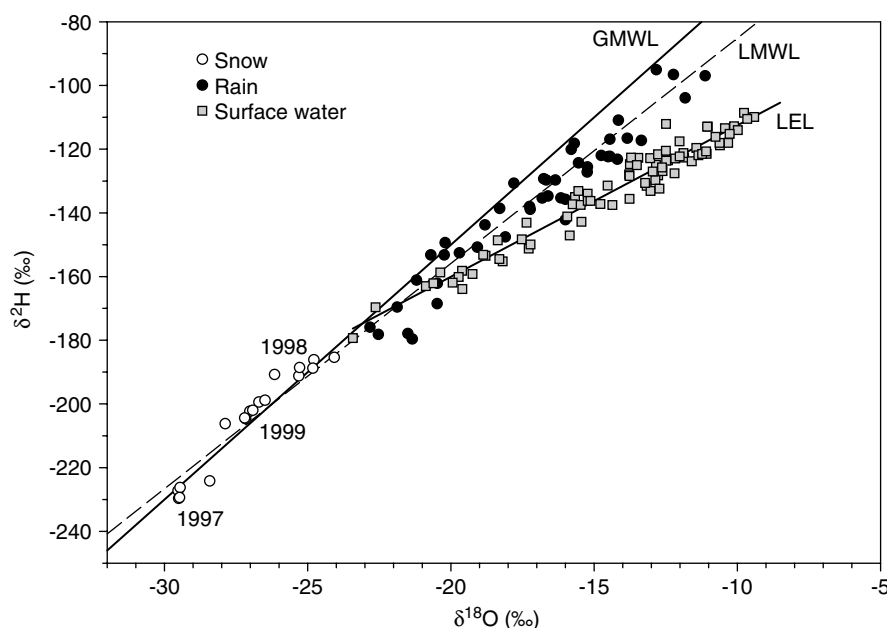


Figure 2. Plot of $\delta^{18}\text{O}$ versus $\delta^2\text{H}$ showing precipitation (snow and rain) and surface water (wetlands and lakes) for the Fort Simpson area. Snow values represent an average from each catchment for a particular year. Note that the distribution of precipitation along the local meteoric water line (LMWL), with a linear relation of $\delta^2\text{H} = 7.1\delta^{18}\text{O} - 14.4$ ($r^2 = 0.98$) close to that of the Global Meteoric Water Line (GMWL, $\delta^2\text{H} = 8.0\delta^{18}\text{O} + 10$), representing temperature-dependent control on precipitation formation. Evaporatively-enriched surface waters plot along a local evaporation line (LEL) having a slope of 4.8 ($r^2 = 0.95$) controlled by local hydroclimatic conditions (i.e. temperature, relative humidity, and isotopic composition of ambient moisture)

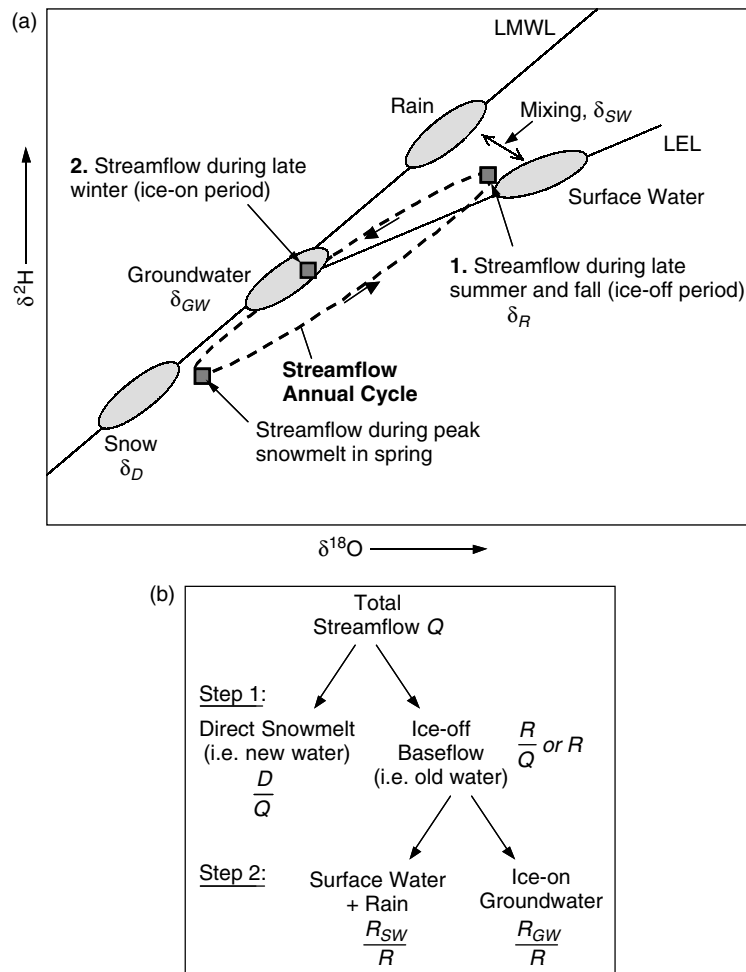


Figure 3. Schematic representation of streamflow partitioning strategy. (a) $\delta^2\text{H}$ – $\delta^{18}\text{O}$ cross-plot illustrating the variation in streamflow isotopic composition over the annual cycle, reflecting various amounts of source water (snow, groundwater, and surface water plus rain) contributions. Source waters are displayed as ovals for simplicity. Numbers 1 and 2 refer to streamflow low-flow isotopic signature that correspond to Band 1 and Band 2 respectively of Figure 4. (b) Flowchart illustrating steps taken in the partitioning strategy. Step 1: total streamflow is partitioned into snowmelt (new water) and baseflow (old water) contributions. Step 2: baseflow is further partitioned into surface water plus rain, and groundwater. See text for complete explanation

at this time. During ice-covered winter periods, progressive reduction of surface water sources and increase in the proportion of groundwater flow leads to a gradual decrease in isotopic signatures towards late winter. In turn, the freshet period is characterized by rapid snowmelt that produces dynamic isotopic shifts from early melt to peak melt, and during the flow recession.

Partitioning of streamflow components

Partitioning of streamflow using stable isotopes as conservative tracers is based on the classical two-component hydrograph separation, and is inferred from the natural cycle of seasonally active source waters (snow, groundwater, surface water) in streamflow, typical of streams in cold climates (Figure 3a). Correspondingly, Figure 4 shows the change in isotope signal of streamflow and discharge hydrographs over a 3 year time-series for each stream in this study. In Figure 4, the average isotopic composition of streamflow

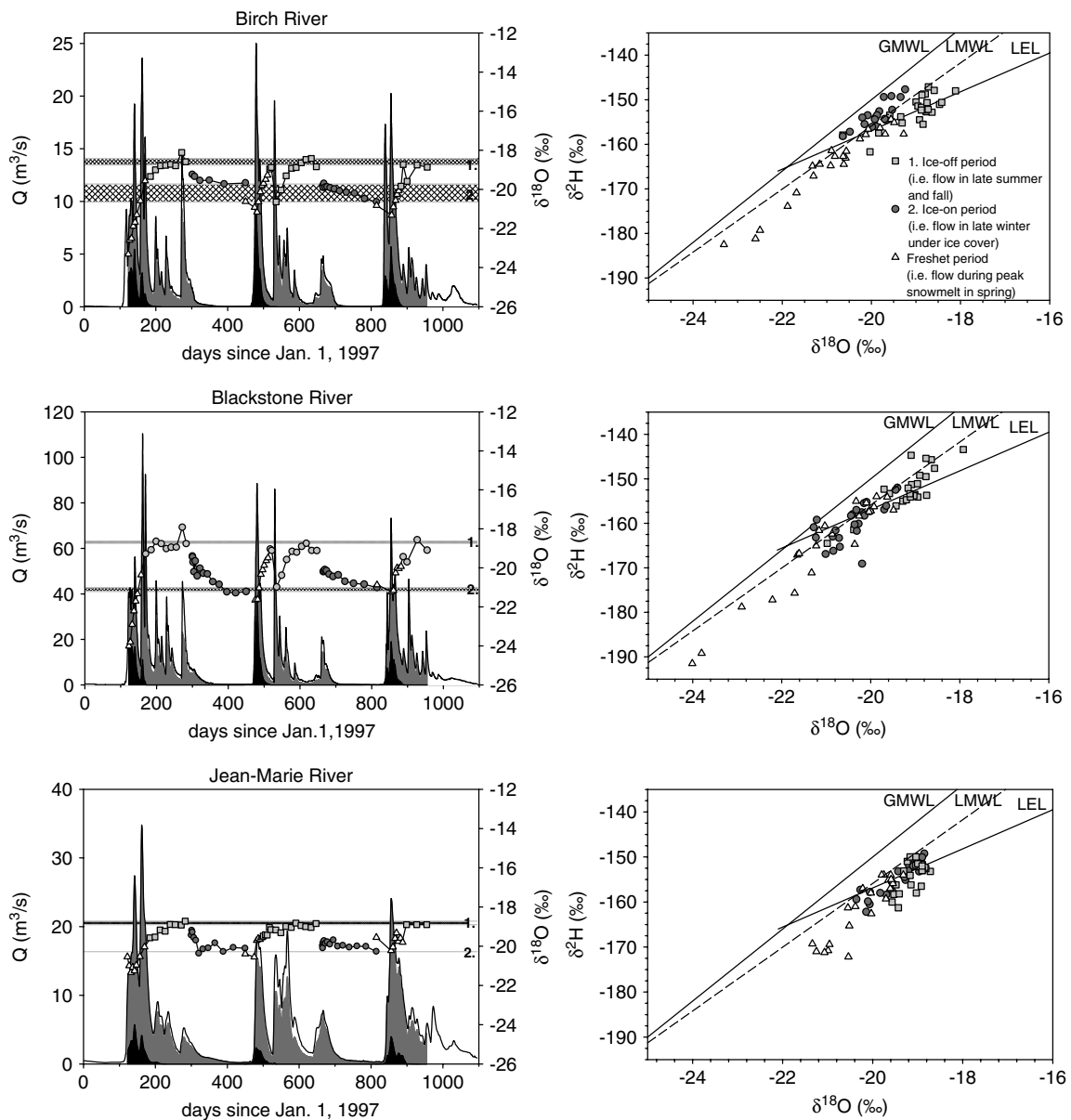


Figure 4. Time-series plots of discharge and isotopic composition of streamflow, and corresponding streamflow variation in $\delta^{18}\text{O}$ – $\delta^2\text{H}$ space for each of the five catchments in the lower Liard basin during 1997–99 period. Black shaded areas under the total discharge curve represent the total amount of snowpack contributing to streamflow; grey shaded areas represent groundwater amounts; white areas depict surface water contributions. The isotopic composition of streamflow is shown using grey filled squares representing ice-off streamflow, dark-grey filled circles represent ice-on streamflow, and empty triangles represent spring freshet. The light-grey bands marked 1 and 2 refer to the range in isotopic limit for ice-off low flow (i.e. flow in late fall prior to freeze-up) and ice-on low flow (flow in late winter under ice cover) respectively. The former is distinguished by the presence of more surface water plus rain, and the latter is dominantly groundwater. The freshet period is initiated by the pulse of snowmelt mixing into streamflow resulting in depleted isotope signatures

during low flow periods is indicated with Bands 1 and 2, respectively representing an upper and lower isotopic limit of streamflow variability. Band 1 indicates the isotopic composition of ice-off low flow (i.e. flow in late fall prior to freeze-up), which includes maximum contributions from surface water and rainfall sources,

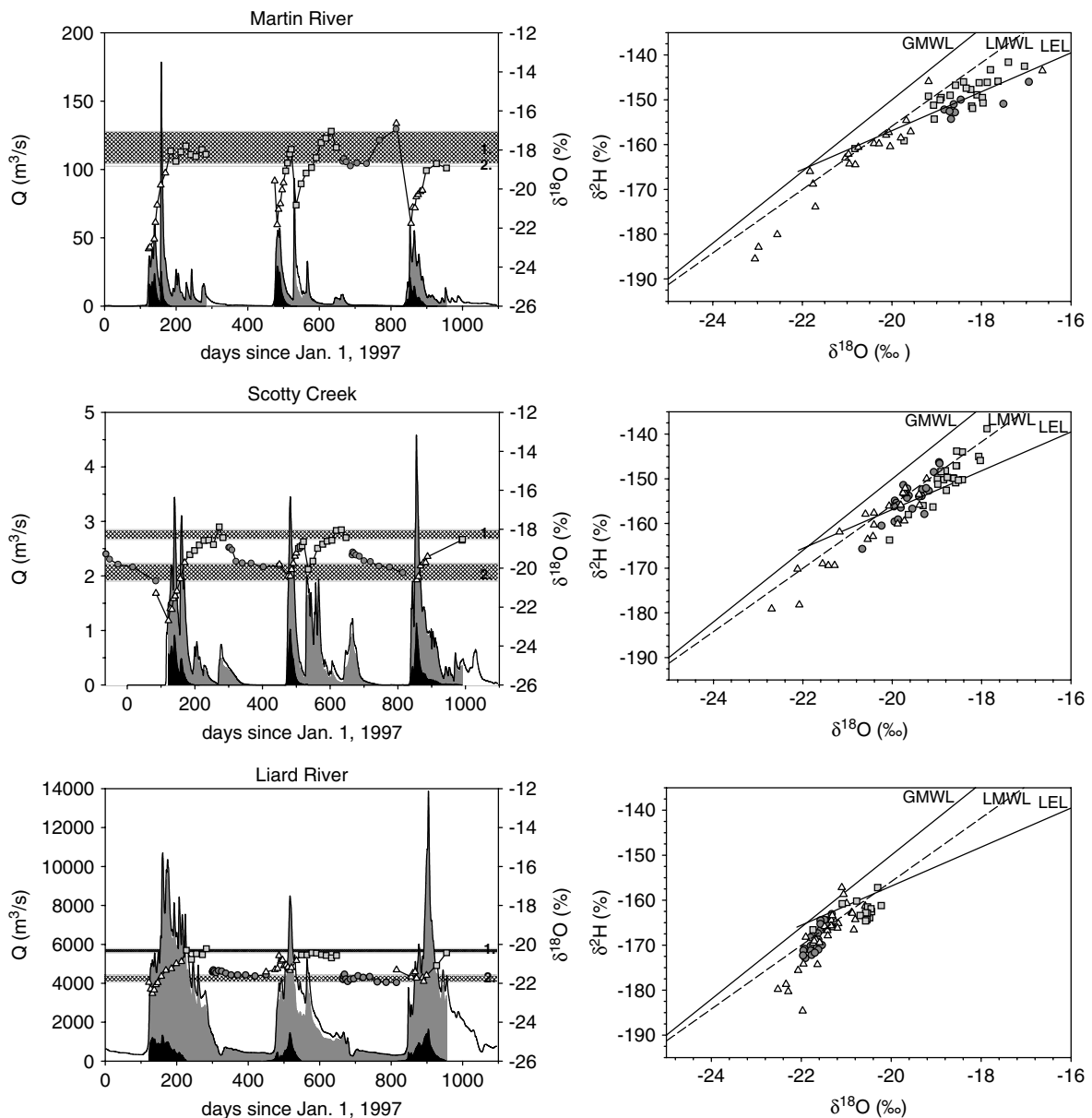


Figure 4. (Continued)

whereas Band 2 refers to the isotopic signal of ice-on low flow (i.e. flow in late winter under ice cover), predominantly provided by groundwater. Accordingly, the proportion of mixing of different source waters in streamflow at any given time is conceptually visualized in $\delta^2\text{H}$ – $\delta^{18}\text{O}$ space, as demonstrated in Figure 3a, thus facilitating source water components to be identified for partitioning.

The mixing ratio between source water components in streamflow is determined in two partitioning steps using mass and isotope balance calculations. The first step in the breakdown of streamflow components involves the partitioning of new and old water, as represented in flowchart form in Figure 3b. During the freshet period, instantaneous contributions of direct snowmelt D (new water), baseflow R (old water, composed

of groundwater and surface water inflows), and direct channel precipitation P to total streamflow Q are given by

$$Q = D + R + P \quad (1)$$

and

$$\delta_Q Q = \delta_D D + \delta_R R + \delta_P P \quad (2)$$

where δ values and subscripts refer to the isotope composition of the respective components.

Direct channel precipitation can be assumed negligible, as most precipitation either recharges to groundwater or enters via surface runoff, and this assumption is especially valid for rain-free periods, or for examining long-term records. In this case

$$Q = D + R \quad (3)$$

and

$$\delta_Q Q = \delta_D D + \delta_R R \quad (4)$$

Substitution of Equation (4) into Equation (3) and rearranging yields

$$\frac{D}{Q} = \frac{\delta_Q - \delta_R}{\delta_D - \delta_R} \quad (5)$$

and

$$\frac{R}{Q} = \frac{\delta_Q - \delta_D}{\delta_R - \delta_D} = 1 - \frac{D}{Q} \quad (6)$$

which are the proportions of new and old water respectively during the freshet recession. The value for δ_R , as shown schematically in Figure 3a, is the isotopic composition of ice-off baseflow represented by Band 1 in Figure 4, which is the most enriched isotopic composition that the stream approaches (i.e. $\delta_R \rightarrow \delta_{SW}$). The initial streamflow signal, characterized dominantly by snowmelt δ_D input, approaches summer baseflow δ_R as the open-water part of the seasonal cycle progresses.

The second step in the breakdown of streamflow components involves partitioning the old water proportion, determined by Equation (6), into groundwater and surface water inflows (Figure 3b), which are dominant components during the post freshet period, when D is negligible during summer to late fall. Accordingly, streamflow has a mass and isotope balance given by

$$R = R_{GW} + R_{SW} \quad (7)$$

and

$$\delta_R R = \delta_{GW} R_{GW} + \delta_{SW} R_{SW} \quad (8)$$

where δ_R is the isotopic composition of baseflow, represented by Band 1 in Figure 4, as before, and $R = R/Q$. By rearranging Equation (7) as $R_{GW} = R - R_{SW}$ and substituting in Equation (8), this yields

$$\frac{R_{SW}}{R} = \frac{\delta_R - \delta_{GW}}{\delta_{SW} - \delta_{GW}} \quad (9)$$

and

$$\frac{R_{GW}}{R} \approx \frac{\delta_R - \delta_{SW}}{\delta_{GW} - \delta_{SW}} = 1 - \frac{R_{SW}}{R} \quad (10)$$

where the R_{SW}/R and R_{GW}/R contributions represent the surface water plus rain and the groundwater respectively. As illustrated in Figure 3a, the isotopic composition of streamflow during late summer is characterized by an enriched isotopic value close to δ_{SW} , which is a mixture of both surface water (lakes and wetlands) and rain that together have an isotopic composition that is difficult to differentiate. Nevertheless, δ_{SW}

spatially characterizes the active (evaporative) components of subsurface and surface runoff. During winter low flow, δ_{SW} approaches the isotopic composition of groundwater (δ_{GW}) as surface water contributions wane. Note that winter streamflow (i.e. when streams are ice covered) is expected to have an isotopic composition close to that of groundwater (Gibson and Prowse, 1999, 2002), where δ_{GW} is represented by Band 2 in Figure 4 and schematically shown in Figure 3a. An exception occurs in the case where streams remain connected to lakes that do not freeze to bottom, and thus receive lake water throughout the winter, as observed for Martin River.

STUDY AREA

This study focuses on five catchments, namely the Birch, Blackstone, Martin, and Jean-Marie rivers and Scotty Creek, ranging in size from 202 to 2050 km², within the lower Liard River basin (277 000 km²) near Fort Simpson, Northwest Territories (61°45'N; 121°14'W), as shown in Figure 1. These catchments are situated within the subhumid mid- to high-boreal ecoclimatic region (Ecoregions Working Group, 1989). Winter climate is characterized by dominance of cold, dry Arctic high-pressure systems; in summer and fall, mild, moist air is brought in by low-pressure systems originating from the Beaufort Sea and Gulf of Alaska. Less frequently, however, low-pressure systems may also originate from the Pacific Ocean, often bringing the heaviest precipitation (Dyke, 2000). The amount of rain that fell during the study period is significantly higher than normal, especially in 1997 (Table I). A similar, higher than normal, trend in temperature is also observed over the 3 years, with 1998 showing the greatest warming (Table I). The trends in precipitation and temperature most likely reflect increased moisture supply (i.e. lower evapotranspiration) and warmer temperatures originating from the tropical Pacific due to a strong El Niño–southern oscillation (ENSO) influence in 1997–98 (Petroni *et al.*, 2000).

The region is influenced seasonally by the strong impulse of snowmelt in late April to early May, coinciding with ice break-up at the Liard and Mackenzie confluence (Prowse, 1986, 1995; Prowse and Marsh, 1989). The hydrographs in Figure 5 reveal a simultaneous response in discharge occurring in all five catchments during the snowmelt period. Rapid loss of snowpack occurs within 1–2 weeks before stream discharge rises; thereafter, rainfall becomes the dominant precipitation. During the post-freshet season, discharge gradually decreases to baseflow levels, punctuated by major rainfall episodes. The timing of major rain events also agrees well with peaks in the discharge curves, reflecting common morphological characteristics and climate conditions over each catchment. The total annual evapotranspiration in the lower Liard River basin is approximately 240 mm over the ice-free period, interpolated from the *Hydrological Atlas of Canada* (den Hartog and Ferguson, 1978). This value agrees well with the average evapotranspiration of 237 mm for the five catchments based on total

Table I. Summary of climate normals for 1971–2000 (Environment Canada, 2002) and for the 1997–99 study period, and land-cover-weighted snow water equivalent (SWE) obtained during snow surveys in late March

	Normals (1971–2000)		Study period (whole year)		
	Whole year	Ice-off season (May–Oct)	1997	1998	1999
Daily mean air temperature (°C)	−3.2	10.3	−1.9	−0.7	−1.7
Total precipitation (mm)	369	260	479	405	431
Total rainfall (mm)	224	220	331	294	228
Total snowfall (mm) ^a	170	n/a	191	175	259
Weighted average SWE (mm)	n/a	n/a	72 ± 10	92 ± 11	96 ± 17

^a Total snowfall estimated for entire winter (i.e. October of previous year to May of following year).

annual precipitation (Table I) minus mean annual discharge (Table II). Hence, adequate potential moisture is available for evaporation and discharge during the ice-off season, and suggests that the residence time of water stored within each catchment is about 1 year.

Typically, the drainage system in the lower Liard basin depends on the relative heights of the water table amongst the distribution of undulating peat plateaus, flat ombrotrophic bogs, and minerotrophic channel

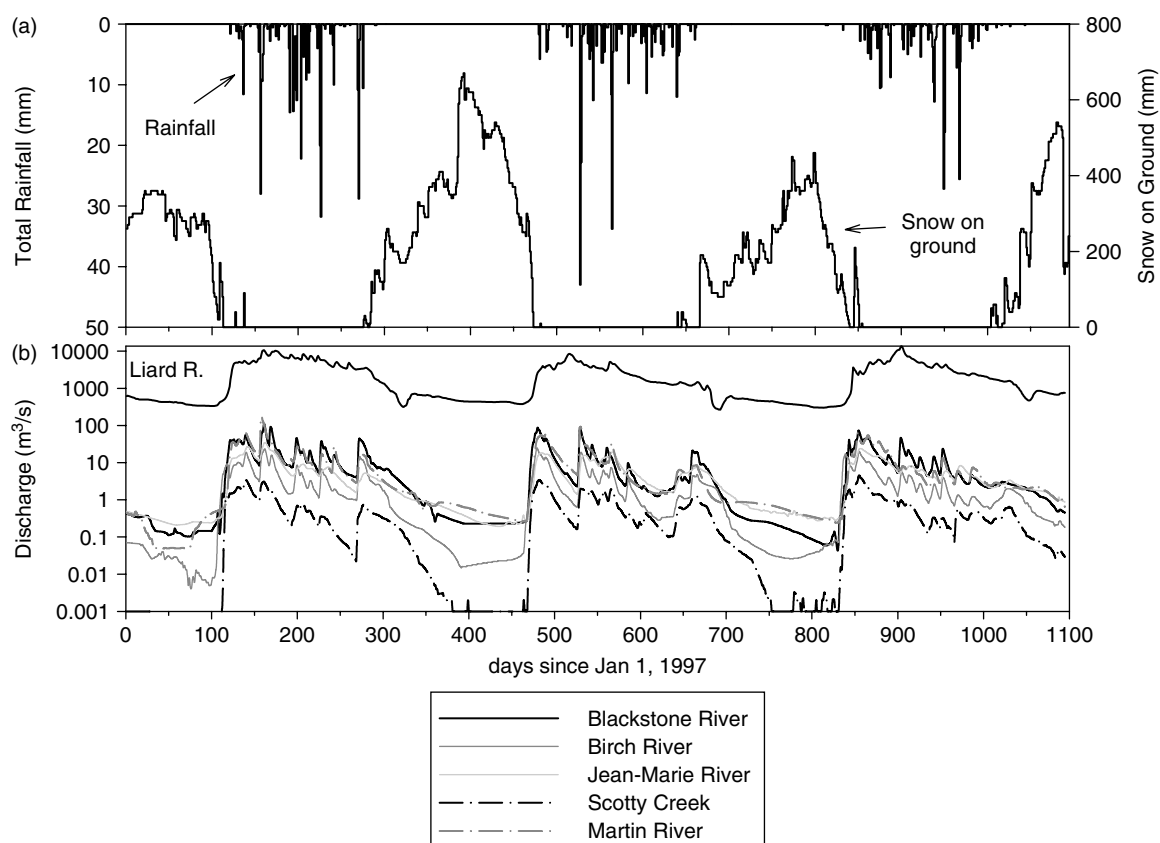


Figure 5. (a) Climate profile of snow and rainfall amounts obtained at Fort Simpson; (b) discharge curves of Liard River and rivers of the five catchments studied (Birch, Blackstone, Jean-Marie, Martin, and Scotty) during 1997–99. The seasonal timing of snowmelt in spring and major rainfall events in summer and fall are reflected in the discharge response of each river

Table II. Mean annual discharge over the period of measurement by Water Survey of Canada and integrated over catchment area to give values in millimetres

Catchment	Measurement period	Mean annual discharge (mm)	Mean discharge during study period (mm)		
			1997	1998	1999
Birch R.	1975–2003	143	172	135	126
Blackstone R.	1992–2003	203	264	179	167
Jean-Marie R.	1973–2003	107	123	111	104
Martin R.	1973–2003	116	161	119	101
Scotty Creek	1995–2003	91	70	81	72

Table III. Percentage of land classification units and gradient for each of the five catchments near Fort Simpson. Land types classified as shrubs, burned and barren are excluded from table since these areas occupy about less than 3% of catchment area

Catchment	Area (km ²)	Basin gradient (%)	Land cover classification (%)					
			Water	Wetland	Transitional	Conifer	Mixed	Deciduous
Birch R.	542	0.5	0.5	24	38	9	18	9
Blackstone R.	1390	0.63	0.7	21	39	14	17	7
Jean-Marie R.	1310	0.3	1.3	14	31	23	22	5
Martin R.	2050	0.7	1.7	18	35	20	7	16
Scotty Creek	202	0.2	2.4	13	43	30	7	3

fens. The proportion of fen to bog coverage increases towards the mouth of the Liard River near Fort Simpson (Aylsworth and Kettles, 2000). Accordingly, Jean-Marie River and Scotty Creek catchments contain areas with extensive fen peatlands, whereas Martin River catchment contains fen-dominated mixed peatland units, situated in a low-lying region around Antoine Lake. Both Birch and Blackstone river catchments are bog-dominated peatlands with little or no fen peatlands present (Aylsworth and Kettles, 2000). Sporadic discontinuous permafrost occurs beneath 10% of the area of which contains moderate ice-content, mainly in areas of thick peat accumulation, shaded north-facing slopes, dry flat bogs and fine-grained till (Rennie *et al.*, 1981; National Wetlands Working Group, 1997; Heginbottom, 2000).

Through the remote-sensing analysis performed by Pietroniro *et al.* (1996), the percentage distribution of different vegetation–terrain classes, generally reflecting moisture conditions, for each catchment has been summarized in Table III, which also includes information on catchment area and gradient. Explicitly, highly elevated, unsaturated peat plateaus are covered mainly by forests of spruce (black and white), jack pine, aspen, birch and alder, low-lying bogs are mostly covered by sphagnum, and fens are vegetated by small shrubs, tamarack, sedges, grasses, and reeds (Zoltai *et al.*, 1988; Gibson *et al.*, 1993b; Reedyk *et al.*, 1995). The transitional forest land-cover type, which is the most prominent vegetation–terrain type in boreal wetland regions, consists of shrubs and deciduous varieties, and immature (i.e. early generation) spruce. The percentage of wetlands listed in Table III comprises fens and bogs as a whole, but its specific distribution within Liard River basin is extrapolated from the Geological Survey of Canada peatland distribution map (Aylsworth and Kettles, 2000). Notably, catchments containing predominantly fen peatlands (i.e. Jean-Marie, Scotty Creek, and Martin rivers) have the highest percentage of open water and total forested cover. Conversely, Birch and Blackstone river catchments have the highest percentage of wetland cover (bog mostly), which coincides with a smaller percentage of forest cover.

The stratigraphy commonly consists of a thick accumulation of organic peat deposited over extensive areas of poorly drained lacustrine (silt and sand) sediments, which overlie poorly drained glacial deposits (till), below which lie clay deposits (Aylsworth *et al.*, 2000). Jean-Marie River and Scotty Creek catchments contain glaciofluvial (sand and gravel) deposits that commonly occur in channels, where subsurface drainage is dominant. For Birch and Blackstone river catchments channels tend to be poorly to moderately drained alluvial (sand, silt, clay, and minor gravel) deposits. To the west side of Liard River, Martin River catchment is characterized by colluvial and till overlying bedrock, and the drainage from mountainous regions is greatly influenced by increasing topographic gradients.

METHODS

Extensive sampling took place during 1997–99 on behalf of the Mackenzie GEWEX Study of the Global Energy and Water Experiment (GEWEX; Stewart *et al.*, 1998). Sampling of streamflow, rain, and surface waters (wetland and lakes) was conducted during the open water season, with the intensity of sampling

greatest during spring to ensure significant capture of seasonal input. Streamflow and rain samples were measured at gauging stations. Snow surveys, encompassing measurements of SWE, observations of land-cover type, and collection of snowpack using a depth-integrated snow sampler, were conducted in late March 1997–99, when snow thickness was at a maximum. Isotopic fractionation during melting or evaporation (or sublimation) of the snowpack is assumed negligible. Daily discharge measurements of Liard River and the five streams were maintained by the Water Survey of Canada. Climate data were recorded at a Class-A synoptic weather station at Fort Simpson airport.

The use of oxygen and hydrogen stable isotopes as conservative tracers in hydrologic studies is based upon systematic differences in the relative abundance of two, rare, heavy isotopic species of water ($^1\text{H}_2^{18}\text{O}$, $^1\text{H}^2\text{H}^{16}\text{O}$) with respect to the common, light species ($^1\text{H}_2^{16}\text{O}$) arising from phase changes and mixing as water passes through the hydrological cycle. Isotopic compositions of ^{18}O and ^2H are expressed in δ notation representing deviations in per mil (‰) from the standard, Vienna standard mean ocean water (VSMOW), such that $\delta_{\text{sample}} = 1000(R_{\text{sample}}/R_{\text{VSMOW}}) - 1$, where R is $^{18}\text{O}/^{16}\text{O}$ or $^2\text{H}/^1\text{H}$. Accordingly, standard analysis of $\delta^{18}\text{O}$ and $\delta^2\text{H}$ is reported with respect to VSMOW on a scale normalized such that $\delta^{18}\text{O}$ and $\delta^2\text{H}$ of standard light Antarctic precipitation has values of -55.5‰ and -428‰ respectively (see Coplen (1996)). All samples were analysed for $\delta^2\text{H}$ and $\delta^{18}\text{O}$ at the University of Waterloo, Environmental Isotope Laboratory. Maximum analytical uncertainties of δ values are $\pm 0.1\text{‰}$ for $\delta^{18}\text{O}$ and $\pm 2\text{‰}$ for $\delta^2\text{H}$.

To achieve a continuous isotopic time-series of streamflow over annual cycles in remote subarctic regions, the isotope stratigraphy of river ice, extracted during late March of 1998 and 1999 (Gibson and Prowse, 1999; Prowse *et al.*, 2002) is used to reconstruct the isotopic composition of winter streamflow (as shown in Figure 4 time-series), based on the equilibrium ice–water isotopic fractionation of $2.93 \pm 0.52\text{‰}$ for oxygen and $17.9 \pm 5.2\text{‰}$ for hydrogen between basal ice and mid-depth water.

RESULTS AND DISCUSSION

Isotopic composition of streamflow components

Surface waters and rain. The isotopic compositions of rain and surface waters (lakes and wetlands) sampled in the five catchments during the 1997–99 study period are shown in Figure 2, and mixing of both defines a value for δ_{SW} in partitioning of streamflow (see Figure 3a and Table IV). Surface waters over the study period have an average composition of -12.9‰ for $\delta^{18}\text{O}$ and -126‰ for $\delta^2\text{H}$ ($n = 64$). During the open-water seasons, the distribution of surface waters plots along the LEL generating an observed slope of 4.8 ($r^2 = 0.95$), as reported by Gibson and Prowse (2002), and is consistent with previous studies in Manners Creek during 1989–90, with a slope of 5.0 (Gibson *et al.*, 1993a). The consistency of the LEL slopes over the long term reflects the prevailing influence of local atmospheric conditions (i.e. relative humidity, temperature, and the isotopic composition of ambient atmospheric moisture) over the region. In essence, the evaporative isotopic enrichment in surface waters is a sensitive indicator of water balance, specifically in defining evaporation: inflow ratios (Gibson and Edwards, 2002; Gibson *et al.*, 2002). Hence, the trend towards increasing enrichment along the LEL corresponds to greater evaporative losses than total liquid inflow.

Rain samples from the lower Liard basin plot in a linear trend below the GMWL, described by $\delta^2\text{H} = 8\delta^{18}\text{O} + 10$, forming an LMWL having a slope of 7.1 (Figure 2). Over the 3 years, the isotopic signature of rain samples has a weighted average of $\delta^{18}\text{O}$ and $\delta^2\text{H}$ of -17.8‰ and -140‰ respectively ($n = 45$). Certainly, the isotopic composition of rainfall is highly variable on a time scale of several days to several weeks, reflecting synoptic-scale variations in local climate. For example, on 5 June 1998, rain had $\delta^{18}\text{O}$ of -11.5‰ and 6 days later rain had $\delta^{18}\text{O}$ of -22.7‰ . Note in Table IV that δ_{SW} for 1998 is more depleted in the heavy isotopes relative to other years due to the incorporation of the latter rainfall event. Relatively large rainfall events (>40 mm) result in a quick response in the isotopic signal in streamflow, such as the 1998 rainfall episode (-22.7‰ ; ~ 70 mm), which produced a strong depleted isotope signal in streamflow (Figure 4). In addition, a large rainfall event (~ 42 mm) on 29 September 1997 had a more

Table IV. Average isotopic composition of streamflow components for each year. Standard deviation for snowpack, baseflow and groundwater reflects variation between catchments

Streamflow component	1997			1998			1999		
	$\delta^{18}\text{O}$ (‰)	$\delta^2\text{H}$ (‰)	<i>d</i> -excess (‰)	$\delta^{18}\text{O}$ (‰)	$\delta^2\text{H}$ (‰)	<i>d</i> -excess (‰)	$\delta^{18}\text{O}$ (‰)	$\delta^2\text{H}$ (‰)	<i>d</i> -excess (‰)
Weighted snowpack δ_D	-29.3 ± 0.7	-228 ± 5	6	-25.0 ± 0.7	-188 ± 5	12	-26.8 ± 1.3	-201 ± 9	14
Baseflow (ice-off low-flow) δ_R	-19.0 ± 0.3	-152 ± 3	0	-18.9 ± 0.2	-152 ± 2	-1	-19.2 ± 0.3	-152 ± 3	2
Weighted rain + surface water, δ_{SW}	-14.6 ± 1.0	-127 ± 7	-10	-17.0 ± 0.8	-143 ± 4	-7	-14.5 ± 0.9	-125 ± 4	-8
Groundwater (ice-on low-flow), δ_{GW}				-20.5 ± 0.8	-158 ± 5	7	-20.4 ± 1.0	-161 ± 7	3

enriched isotopic signature of -12.8‰ ($\delta^{18}\text{O}$), most likely associated with an air mass originating from tropical regions of the Pacific Ocean (Lawrence and White, 1991), whereas isotopically depleted rain may be derived from low-pressure systems originating from the North Pacific and Arctic Oceans. As suggested by the reduced interbasin variability of the isotope signal of rain, all catchments may be influenced under similar atmospheric conditions. Unfortunately, large rain events with an isotopic composition similar to that of baseflow are not detectable in streamflow isotopic signature, but they are evident in discharge curves.

Snow. The average isotopic values of snowpack in the $\delta^2\text{H}-\delta^{18}\text{O}$ plot for each catchment scatter mainly in three groups along the LMWL (Figure 2), showing interannual variability associated with mean annual temperature. Similarly, in Figure 6, significant year-to-year variability in SWE, obtained during snow surveys in the lower Liard River basin, is also observed. Low mean annual temperature in 1997 (Table I) corresponds with snowpack samples that are significantly depleted in $\delta^{18}\text{O}$ and $\delta^2\text{H}$ (and plot slightly below the LMWL in Figure 2), as well as having low and tightly constrained SWE values (Figure 6). In contrast, the above-normal mean annual temperature in 1998 corresponds with snowpack samples having appreciably enriched isotopic compositions, as observed by the more positive shift along the LMWL (Figure 2) and greater spread in SWE (Figure 6). Although the mean annual temperature for 1999 was similar to that of 1997 (Table I), there was considerably more snowfall in 1999, possibly leading to similar trends in SWE and isotopic composition of snowpack as the 1998 samples (Figure 6).

Melting and refreezing of the snowpack is not likely to occur over the winter season in subarctic regions given the low temperatures, and sampling in 1997 and 1998 was conducted before snowmelt initiated; hence, the isotopic values and accumulation are likely to be representative of the snow characteristics in the area. In 1999, daily mean temperature reached above 0°C on 19 March for six consecutive days before start of sampling on 24–29 March. Some snowmelt fractionation may have occurred (Moser and Stichler, 1980; Herrmann *et al.*, 1981; Cooper, 1998; Taylor *et al.*, 2001); however, considering the placement of the 1999 snowpack isotopic signal in $\delta^2\text{H}-\delta^{18}\text{O}$ space relative to the more enriched 1998 snowpack (Figure 2), the 1999 snowpack may not have undergone significant enrichment. However, the 1999 snowpack may have minor sublimation loss, as deduced by the position slightly above the LMWL (Figure 2), and may be responsible for the spread in SWE values (Figure 6) and higher d -excess (Figures 6 and 7).

Variations in snow d -excess ($d = \delta^2\text{H}-\delta^{18}\text{O}$) and SWE values with vegetation cover (i.e. forested versus open areas) primarily reflect the controlling function of plant density and terrain characteristics on snow distribution (Yang and Woo, 1999), as demonstrated in Figure 7. The isotopic composition of snowpack δ_D (Table IV) used in partitioning streamflow during the freshet period (see Figure 3a) is weighted according to land-cover type. The weighting reduces the bias associated with sampling over certain types of vegetation cover, which exerts a significant control on snow redistribution. In forested areas, conifer canopies are considerably efficient at intercepting snow, which is mainly subjected to sublimation rather than falling to the ground (Hedstrom and Pomeroy, 1998). In addition, increased forest density shelters snow on the ground from incoming solar radiation and wind ablation (Woo and Heron, 1987; Marsh, 1990), so that, on average, SWE values of samples collected in forested areas are generally lower and d -excess is correspondingly higher than other land-cover types (Table III), as discerned from Figure 7. The high SWE values observed for transitional forest cover (Figure 7) and by Woo and Heron (1987) reflect deep snow cover due to drifting. In open areas (i.e. lakes and wetlands), snow d -excess and SWE values generally reflect areas that receive maximum wind exposure and solar radiation. As shown in Figure 7, SWE values are higher and snow d -excess are lower in lake and wetland areas than values in vegetated areas. Evidently, snow density can increase considerably for well-exposed areas (Male and Gray, 1981; Woo and Heron, 1987; Pomeroy *et al.*, 1998), and Schotterer *et al.* (2003) have observed a decline in d -excess by 10‰ over the course of intense sublimation. Snow accumulation over ice may result in subsidence of the ice cover during the course of the winter season, resulting in the assimilation of lake water into the snowpack, further increasing the spread of SWE, and especially affecting d -excess values between the 3 years, as observed for 1998 sample (Figure 7).

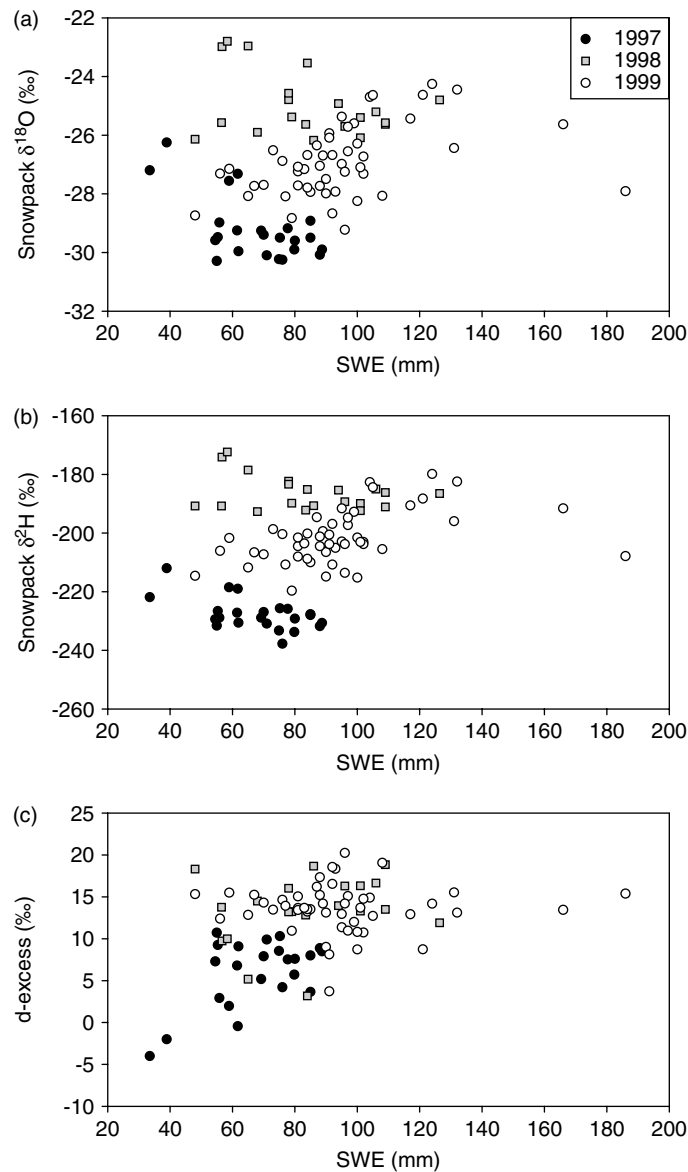


Figure 6. Plots of (a) $\delta^{18}\text{O}$, (b) $\delta^2\text{H}$ and (c) d -excess of snowpack versus SWE showing interannual variability in the snow samples from the five catchments. An orderly shift towards isotope enrichment and greater SWE values is observed

The observed spatial and temporal variations in SWE and isotopic composition of snow are slightly manifested among bog-, fen- and lake-dominated catchments. In essence, Jean-Marie and Scotty Creek river catchments, both having the largest percentage of forest cover (Table III) and associated fens, have low average land-cover-weighted SWE (1997: 70.81 mm; 1998: 91.25 mm; 1999: 95.20 mm) and high d -excess values (1997: 6.53‰; 1998: 11.70‰; 1999: 13.62‰). By comparison, Blackstone and Birch river catchments, having a larger percentage of open wetland (bog) coverage, generally have high SWE (1997: 71.91 mm; 1998: 92.79 mm; 1999: 96.01 mm) and correspondingly low d -excess values (1997: 6.36‰; 1998: 11.34‰; 1999: 13.48‰). The differences in d -excess and SWE between bog- and fen-dominated catchments are rather small

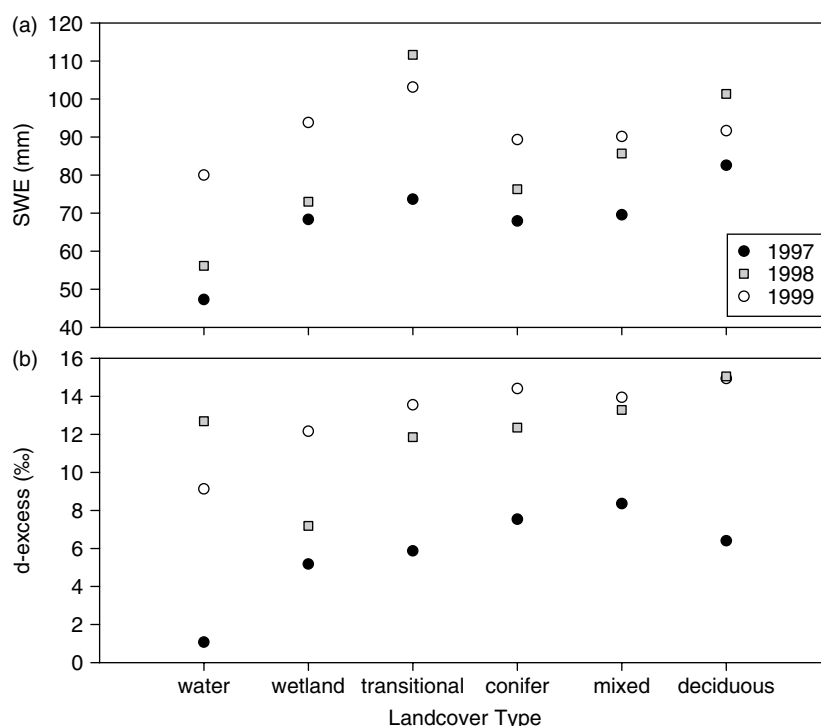


Figure 7. Plots of (a) SWE and (b) d -excess averaged and sorted according to land-cover type for snowpack sampled within the five catchments during late winter, 1997–99. Note the consistency of trends in both SWE and d -excess for each land-cover type over the three sampling years, with year 1998 having more pronounced variability

(i.e. 0.14–0.36‰), but still above the analytical uncertainty of 0.1‰ for ^{18}O , thus stressing the importance of prevailing atmospheric influence and the controlling role of vegetation type on distribution of snow. The weak, but apparent, d -excess–SWE relationship may be quantifiable in future studies, and hence provide a unique tool for identifying snow depositional processes and detecting moisture sources (Gat *et al.*, 1994). Note, both the 1998 and 1999 snow d -excess and land-cover-weighted SWE values are higher than those of 1997 (Figure 7). The high d -excess value in 1998 may be associated with elevated moisture transport from the Pacific Ocean during an El Niño phase, since interannual variability in SWE was shown to correlate with the phases of ENSO (Cayan, 1996).

Temporal and spatial isotope variability of streamflow

Isotopic evolution of streamflow in $\delta^2\text{H}$ – $\delta^{18}\text{O}$ space. The seasonal evolution in $\delta^{18}\text{O}$ of streamflow is illustrated by the isographs and $\delta^2\text{H}$ – $\delta^{18}\text{O}$ cross-plots in Figure 4 for each catchment. Similar trends are also noted in $\delta^2\text{H}$ of streamflow, but are not shown. After input of isotopically depleted snow at the peak spring melt period, the isotopic composition of post-freshet streamflow evolves towards Band 1. Streamflow isotopic values are also shown to migrate closely along the LEL in $\delta^2\text{H}$ – $\delta^{18}\text{O}$ space as enriched surface water plus rain contributions increase, as shown in Figure 4. Noteworthy deviations from the LEL trend are due to varying amounts of input of groundwater and rain mixing into streamflow. During the winter, streamflow isotopic values plot towards a groundwater isotopic composition that is close to the intersection of LEL and LMWL.

Significant differences in seasonal variation of isotopic composition of streamflow are apparent between the five catchments. These differences reflect varying distribution of bog and fen peatlands and lakes within each catchment. For instance, during the snowmelt period, bog-dominated (i.e. Birch and Blackstone

rivers) and lake-dominated (i.e. Martin River) catchments show strong depletion in isotopic composition of streamflow, indicating a significant input of snowmelt, as shown by the large spread in freshet streamflow values in $\delta^2\text{H}$ – $\delta^{18}\text{O}$ space (Figure 4). In contrast, fen-dominated catchments (i.e. Jean-Marie River and Scotty Creek) show both freshet and ice-off streamflow isotopic values more constrained around the LMWL–LEL intersection, reflecting a dominant groundwater regime. Likewise, Liard River streamflow has very little seasonal variation in isotopic composition because of drainage through a larger basin area that encompasses greater heterogeneity in land surface features that include alpine sources, and hence plot well below the intersection of LMWL–LEL.

Baseflow (ice-off low-flow). By late July through to early October the discharge reaches baseflow (i.e. ice-off low-flow) levels in each catchment, and progressive enrichment in heavy isotopes occurs as the proportion of surface water plus rain contribution δ_{SW} increases. Spatial variability in baseflow δ_R , denoted as Band 1 in Figure 4 and summarized in Table IV, is rather small, and even seepage collected in Manners Creek (see Figure 1) during the 1998 open-water season also shows very similar isotopic compositions in both ^{18}O and ^2H (average -18.7‰ and -156‰ respectively).

Groundwater (ice-on low-flow). With a significant decrease in stream discharge volume over the winter, isotopically enriched surface water contributions decline and groundwater isotopic signal predominates streamflow composition by the end of winter. The isotope composition of streamflow during late winter under ice cover (i.e. ice-on low-flow) identifies the groundwater source component δ_{GW} value used in the second step of the streamflow partitioning strategy (see Figure 3). Values for 1998 and 1999 δ_{GW} are summarized in Table IV and depicted as Band 2 (groundwater, δ_{GW}) in Figure 4. Gibson *et al.* (1993b) obtained an isotopic composition of -20.7‰ ($\delta^{18}\text{O}$) and -168‰ ($\delta^2\text{H}$) for icings, and -20.6‰ ($\delta^{18}\text{O}$) and -164‰ ($\delta^2\text{H}$) for groundwater in a 1990 study within Manners Creek tributary, thus demonstrating considerable temporal and spatial stability in isotopic signals of groundwater. Hence, an average value for δ_{GW} was applied for years without ice-reconstructed data. However, Martin River's streamflow isotopic composition for ^{18}O (and ^2H , not shown) during the winter reaches a value more enriched than the average isotopic composition of 1998 δ_{SW} (i.e. $\delta_{\text{GW}} > \delta_{\text{SW}}$), and this is attributed to input of isotopically enriched lake water into streamflow by late winter, possibly due to snow loading effects (Adams, 1981; Gibson and Prowse, 2002). Therefore, δ_{SW} used in partitioning Martin River's streamflow is redefined to reflect input water from Antoine Lake (-9‰ , -108‰).

Hydrograph characteristics

The shape of the hydrograph contains significant qualitative information about the temporal and spatial variability of water input, storage effects, vegetation distribution, and pathway mechanisms, which often reflect differences in antecedent moisture conditions and connectedness of water bodies within a catchment (Price, 1987; Quinton and Roulet, 1998). Dissimilarities in hydrograph characteristics become readily apparent between bog-dominated catchments (i.e. Birch and Blackstone rivers) and fen-dominated catchments (i.e. Jean-Marie River and Scotty Creek), as shown in Figure 4. For instance, Birch and Blackstone rivers have sharp, well-defined peaks representing quick response to runoff events due to high moisture content and reduced infiltration rates, and thus connectivity between water bodies may persist for extended periods. In comparison, Martin River hydrograph also shows similar sharp peaks, demonstrating comparable runoff response associated with both lake and mixed peatland morphological characteristics. By contrast, Jean-Marie River and Scotty Creek hydrographs show broad peaks (Figure 4), suggesting high infiltration rates and longer response and recession times, which are attributable towards the slow release of water from thick peat accumulations in fens and peat plateaus that have large water-retaining capacity (Dingman, 1973).

Specific similarities between bog- and fen-dominated catchments in timing of snowmelt and discharge response are noted. The 1997 snowmelt peak (as indicated by the first rise in the discharge curve) for Birch,

Blackstone, and Martin rivers occur between 28 April and 5 May, followed by Scotty Creek on 10 May, and then Jean-Marie River responding to snowmelt much later on 22 May (Figure 4). In response to above-average air temperatures, an earlier snowmelt peak in 1998 occurs in all five catchments between 24 and 30 April, with bog-dominated catchments showing the earlier response, and Jean-Marie River, being fen-dominated, exhibiting the latest peak time. The 1999 snowmelt peak occurs approximately 3–6 May for all five catchments, again with Jean-Marie River having its snowmelt maximum occurring later than the other catchments. Note, for bog-dominated catchments, the rainfall events that occur later show as being very responsive during the spring (as moisture conditions are still relatively high), whereas fen-dominated catchments demonstrate slower responses (as shown by smaller peak heights) to snowmelt and rainfall events, thus implying higher infiltration rates and storage capacity (Quinton and Roulet, 1998). Equally important to note is that the Liard River hydrograph shows similarities in isotopic response of source waters to streamflow compared to the smaller five catchments, mitigating the applicability of using isotopes in partitioning streamflow for larger scale river basins.

Streamflow contributions

The partitioning results of streamflow into source-water components reveal significant groundwater contributions throughout the annual cycle, as illustrated by the grey shaded portion under the total discharge curves of Figure 4. On average, over the 3 years, partitioning of streamflow using either $\delta^{18}\text{O}$ or $\delta^2\text{H}$ reveals that between 54 and 79% of groundwater contributes to streamflow during the freshet period. This percentage range corresponds well with the estimate of 50–60% reported by Gibson *et al.* (1993b) for streamflow accounted as groundwater in the Manners Creek watershed (see Figure 1). Correspondingly, Hayashi *et al.* (2004) estimated maximum snowmelt contributions of 41% in 2000 and 56% in 2002 for Scotty Creek, which are higher than the 31–33% snowmelt contributions obtained in this study (Table V), generally reflecting greater SWE in 2000 and 2002 than during the 1997–99 period (see Tables I and II). Overall, there is good agreement between the two stable isotope tracers in determining the snowmelt component for the 1997–99 period ($r^2 = 0.92$; Figure 8), demonstrating that $\delta^{18}\text{O}$ and $\delta^2\text{H}$ of source waters contribute to streamflow through the same pathways, as both tracers behave conservatively. As the ice-off season proceeds, the snowmelt component diminishes from the total discharge and the surface water plus rain becomes an increasingly important source contribution until late summer and fall. Certainly, the average groundwater component has remained a significant contributor throughout the baseflow period, being about 7% greater than during the spring. In comparison, the agreement between tracers for the surface water plus rain component

Table V. Source water contributions for 1997–99. Maximum snowmelt refers to peak spring melt contribution to total streamflow. Maximum surface water contribution takes place just before the end of the baseflow period in early fall. Surface water contributions also include rainfall runoff. Average uncertainty derived from Genereux (1998) equation for groundwater fraction

Catchment	Freshet period				Post-freshet period							
	Maximum snowmelt contribution D (%)		Uncertainty (%)		Maximum surface water R_{SW} (%)		Average surface water R_{SW} (%)		Average groundwater R_{GW} (%)		Uncertainty (%)	
	$\delta^{18}\text{O}$	$\delta^2\text{H}$	$\delta^{18}\text{O}$	$\delta^2\text{H}$	$\delta^{18}\text{O}$	$\delta^2\text{H}$	$\delta^{18}\text{O}$	$\delta^2\text{H}$	$\delta^{18}\text{O}$	$\delta^2\text{H}$	$\delta^{18}\text{O}$	$\delta^2\text{H}$
Birch R.	37	34	3	6	39	51	29	21	71	79	11	21
Blackstone R.	40	41	4	7	48	61	36	39	64	61	10	24
Jean-Marie R.	21	21	2	6	32	35	29	28	71	72	9	20
Martin R.	46	44	4	6	27	39	14	20	86	80	7	19
Scotty Cr.	31	33	3	6	42	60	30	34	70	66	10	26
Liard R.	20	24	3	8	22	24	20	20	80	80	6	16

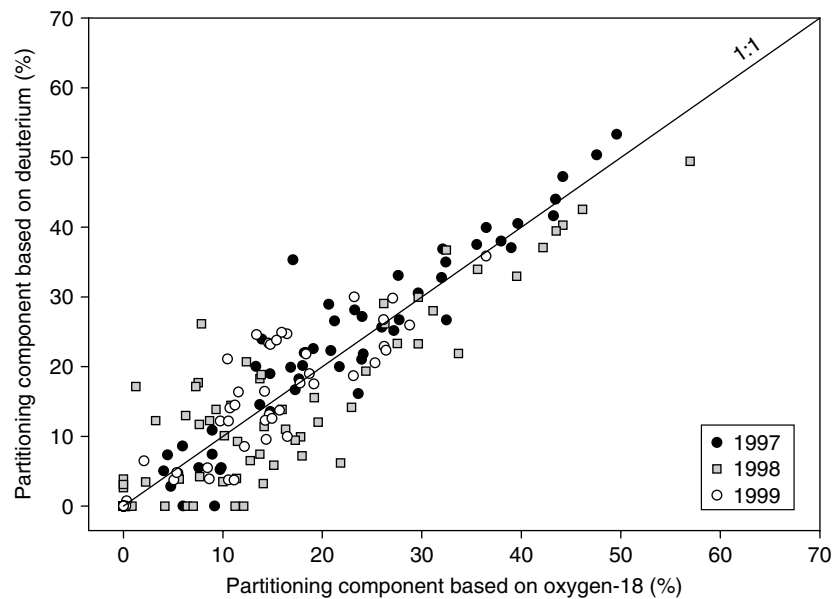


Figure 8. Results from partitioning of snowmelt component based on ^2H (%) versus ^{18}O (%) for all catchments during 1997–99. Good agreement between the two tracers, with a linear regression of $r^2 = 0.92$, suggests that the isotope-mass balance model used for isotopic separation of streamflow during the freshet period adequately represents the natural system

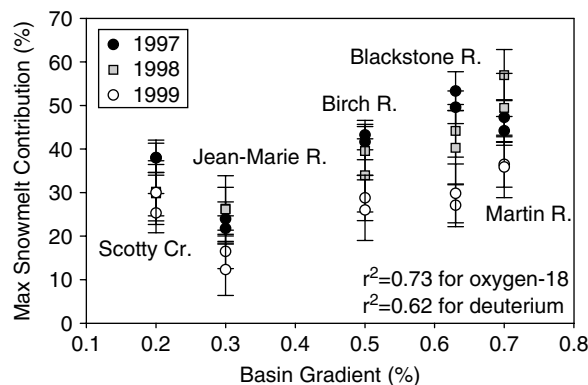


Figure 9. Plot of maximum snowmelt contribution (%) versus basin gradient for each catchment. Note that the positive trend between snowmelt contribution and gradient is observed for each year. Percentage contributions determined from both ^{18}O and ^2H are shown

shows slightly more scatter about the linearity line than during spring melt, generating $r^2 = 0.57$ (not shown), which may be attributable to evaporative enrichment effects of surface water isotopic composition.

Freshet period. As shown in Figure 9, the percentage of snowmelt contributing to streamflow during the spring peak period over the 3 years has a modest linear correlation with basin gradient, in spite of the fact that all catchments are relatively flat, with a gradient of less than 1% (Table III). Generally, increased basin gradient leads to higher percentage of snowmelt runoff and a decrease in contribution of groundwater fraction by the same amount. Because of low gradients, this relation is obviously overprinted by effects of land-cover characteristics on snowmelt runoff (Price, 1987), as illustrated by the deviation of Scotty Creek from the positive trend in Figure 9.

Woo and Heron (1987) have demonstrated that differences in land cover lead to variation in snowmelt rates, with open areas promoting quick snowmelt and direct runoff over frozen saturated ground, and forested areas contributing to snowmelt attenuation and infiltration. Based on available land-cover-weighted SWE (Table I), the total runoff that could be generated over wetland versus conifer-dominated forest cover is presented in Figure 10 for each catchment. Significant runoff can be generated from open wetland (mostly bog) areas in Birch and Blackstone river catchments, whereas both wetland (mostly fen) and forested areas provide possible source areas for snowmelt generation in Jean-Marie River and Scotty Creek catchments (Figure 10). Accordingly, the potential snowmelt generated over forest-covered areas in Birch and Blackstone river catchments is not sufficient to explain the observed snowmelt contribution estimates based on isotopic partitioning. However, the extent of forest cover, which is characterized by greater peat accumulation with high infiltration rates, in both Jean-Marie River and Scotty Creek catchments, may help to explain the longer recession observed in the hydrographs during the spring melt period (Figure 4). In addition, the presence of lateral flow of groundwater in these fen-dominated catchments also justifies that snowmelt mixes and displaces a greater proportion of groundwater contributions to streamflow than bog-dominated catchments. The total snowmelt contribution for Martin River is comparable to that of Birch and Blackstone rivers, which suggests that a combination of high basin gradient to the west and open environment (Lake Antoine, wetlands, impermeable tills) may have triggered significant snowmelt runoff.

The difference between SWE and amount of snowmelt contributions in streamflow provides an approximate estimate of water stored in each catchment (Male and Gray, 1981), assuming evapotranspiration and rainfall events are negligible during the freshet period (Figure 10). Blackstone and Martin river catchments have the lowest storage amounts, followed by Birch River catchment, presumably due to a combination of

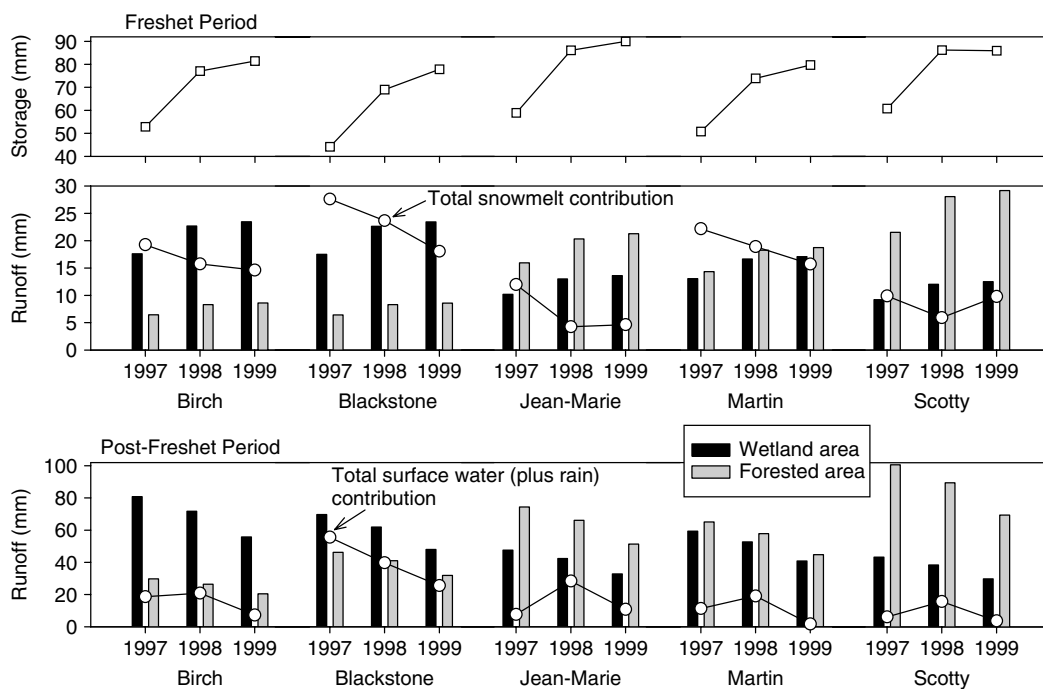


Figure 10. Total streamflow contributions (indicated by open circles) for both freshet and post-freshet periods respectively represent the total snowmelt and surface water (plus rain) runoff as determined from isotopic separation results. Vertical bars indicate the total runoff that could be generated over an area characterized by wetlands (bogs and fens) and forests (conifer dominated) in each catchment, based on the available SWE and total rainfall for each year during the freshet and post-freshet period respectively (Table I). Available storage for each catchment during the freshet period is estimated as the difference between SWE and total snowmelt contribution

impermeable discontinuous permafrost and fine-grained tills (Aylsworth *et al.*, 2000). By contrast, Jean-Marie River and Scotty Creek catchments show the largest storage amounts, consistent with higher peat accumulations associated with the forest regime.

Post-freshet period. Hydrological routing and storage capacity within these wetlands evolve during the post-freshet period as the water table lowers and evapotranspiration rates increase (Quinton and Roulet, 1998). In Figure 10, the total surface water runoff that could be generated from wetland and forested areas is based on total available rainfall (Table I); in comparison with the amount of estimated surface water (plus rain) contributions, both land cover types provide areas for water storage in each catchment. Bog-dominated catchments have higher surface water contributions, as streamflow receives a combination of surface flow and slow subsurface drainage, depending on the initial storage conditions during the spring melt. Apparently, Blackstone River had the least amount of storage capacity in spring and, consequently, resulted in having the greatest surface water (plus rain) contribution during post-freshet season (Figure 10). On the other hand, fen-dominated catchments (i.e. Jean-Marie River and Scotty Creek) will continue to contribute groundwater to streamflow throughout summer and fall via lateral flow, thus suppressing much of the surface water (evaporative input) contribution. Evidently, the small difference of approximately 4% between maximum and average surface water contributions (for both isotope tracers) for Jean-Marie River (and Liard River) exemplifies the importance of steady groundwater flow in this catchment (and Liard River basin), compared with the greater difference of 18% observed for other catchments (Table V). Consequently, the greater difference between maximum and average surface water contribution for Scotty Creek (Table V) may be attributable to variable contributions between upland (bog) and lowland (channel fens) as the hydrological connectivity changes over the post-freshet period (Hayashi *et al.*, 2004). Lastly, as observed in Figure 10, Martin River's total surface water (plus rain) contributions are low, despite the apparent spring melt saturated conditions, implying that the mixed fen-peatland and the presence of Antoine Lake at the lower portion of the catchment may be influencing control in the hydrological regime.

Interannual variability in water balance. In Figure 10, variation in surface water contributions in Blackstone River correspond well with the amount of rainfall (Table I), considering that very little rainfall is necessary to initiate saturation overland flow. A lower surface water contribution in 1997 during the post-freshet period is observed for other catchments. This suggests increased storage availability related to a combination of low SWE amount during the freshet period and high evapotranspiration (i.e. 321 mm, based on average of total precipitation minus mean discharge of the five catchments in Tables I and II) compared with the following years. Note, evapotranspiration decreases by 41 mm in 1998, thus prolonging the moisture supply available for sustaining hydrological connectivity during the post-freshet period. Consequently, high antecedent moisture conditions have enhanced runoff generation (Kane and Stein, 1983) during the 1999 spring melt period, as observed for Scotty Creek and Liard River, and less so for Jean-Marie River (Figure 10). In contrast, increased attenuation of snowmelt runoff in 1999 for Birch, Blackstone and Martin rivers may reflect a decrease in groundwater flow during the 1998–99 winter, especially within bog-dominated catchments (Price and FitzGibbon, 1987).

The percentage of streamflow components for each year is displayed in ternary plots to aid in perception of the overall moisture conditions of each catchment (Figure 11). The year 1997 reflects a decrease in hydrological connectivity (increase in storage) towards the post-freshet season, leading to higher groundwater contributions to streamflow. With the onset of El Niño in 1997–98, the earlier occurrence of snowmelt extended the open-water evaporative season, allowing a combination of longer residence time for isotopic enrichment of surface waters and lower evapotranspiration rates, resulting in a greater proportion of surface water component observed in streamflow. The 1999 snowmelt event occurred at a similar time to that in 1997; however, a combination of higher SWE and lower rainfall amounts in 1999 resulted in a shift towards greater snowmelt and greater surface water contributions respectively, as shown in Figure 11.

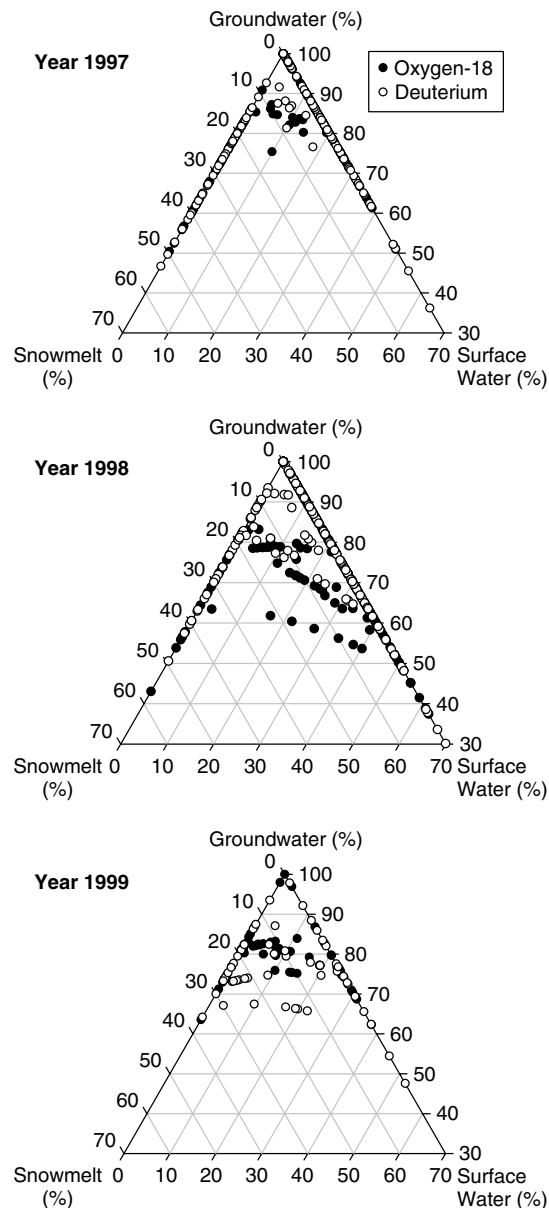


Figure 11. Ternary plots showing streamflow contribution percentages in all catchments depicting water balance conditions for each year. For year1997, low SWE and greater rainfall (and greater storage conditions during post-freshet) lead to an overall displacement of groundwater contribution to streamflow. For year1998, slightly higher SWE and longer open-water season, due to earlier snowmelt timing, lead to a shift towards snowmelt and surface water contributions. Note that seasonal shifts from snowmelt to surface water contributions can be visibly traced out in the 1998 plot, such as the isotopic evolution of streamflow for Blackstone River situated in the centre. Total streamflow components for 1999 show a combination of having the highest SWE and saturated conditions during the freshet period and then a subsequent change to lower rainfall amounts during post-freshet

Error analysis

The partitioning analysis is based on the isotopic composition of source waters and streamflow and of daily discharge rates. Accordingly, the relative accuracy of the partitioning method depends on the determination

of these values. In general, the effectiveness of the separation depends on the isotopic difference between the end components, with error being reduced for larger isotopic differences. The uncertainty in the fraction of groundwater W_G can be determined using the following (Genereux, 1998):

$$W_G = \sqrt{\left[\frac{C_S - C_Q}{(C_G - C_S)^2} W_{CG} \right]^2 + \left[\frac{C_Q - C_G}{(C_G - C_S)^2} W_{CS} \right]^2 + \left(\frac{1}{C_G - C_S} W_{CQ} \right)^2} \quad (13)$$

where W_{CG} , W_{CS} and W_{CQ} correspond to the uncertainties in the isotope concentrations of groundwater (C_G), runoff as snowmelt or surface water (C_S) and sample stream water (C_Q) respectively. The type of uncertainty propagated in W represents the analytical uncertainty plus the standard deviation associated with each component C . For W_{CG} , W_{CS} and W_{CQ} , the analytical uncertainties do not change and are equal to 0.1‰ and 2‰ for $\delta^{18}\text{O}$ and $\delta^2\text{H}$ respectively. On average, the uncertainty in partition estimates for groundwater fraction based on oxygen and hydrogen are a maximum of $\pm 5\%$ and $\pm 8\%$ respectively for the spring melt season (see Table V). Snowmelt fractionation was assumed negligible in this study. However, if significant, then an overestimation of the groundwater fraction would result, and uncertainty would increase to a maximum of $\pm 14\%$ and $\pm 16\%$ for oxygen and hydrogen respectively, assuming the largest difference between the initial snowpack and final meltwater as observed in other studies (Moser and Stichler, 1980; Herrmann *et al.*, 1981; Taylor *et al.*, 2001). For the summer and fall periods the isotopic difference between source components decreases, leading to an average error estimates of $\pm 9\%$ (for $\delta^{18}\text{O}$) and $\pm 21\%$ (for $\delta^2\text{H}$) in the groundwater fraction (see Table V). The greater uncertainty in the summer and fall partitioning results may also be a consequence of merging error generated in the first step of partitioning with error generated in the second step (see Figure 3b). Noticeably, uncertainty in groundwater is greatest during 1998 due to increased surface water contribution.

CONCLUSIONS

The separation of each streamflow component (i.e. snowmelt, surface water and groundwater) is made possible by the seasonally distinctive differences in their isotopic signals, and thus the magnitude and timing of the source waters were determined over annual cycles. Over winter, decline in discharge is usually accompanied by a prominent isotopic shift to compositions reflecting groundwater, which remains spatially and temporally invariant during the study period. At peak runoff in spring, the isotopic composition of streamflow is enhanced by inputs of isotopically depleted snowmelt. Evaporative enrichment of surface waters, plus rainfall runoff, contributes to the total streamflow during the summer thaw season. For the entire annual period, however, groundwater remains the principal source water in streamflow for all catchments.

Significant differences in hydrological responses among bog-, fen- and lake-dominated catchments are apparent in the hydrographs, isotopic composition of streamflow and, consequently, in the partitioning results, which vary according to land cover distribution (e.g. open wetland, forest). Birch and Blackstone river (bog-dominated) catchments had an average of 39% snowmelt contribution to total streamflow, whereas Jean-Marie River and Scotty Creek (fen-dominated) catchments, which are predominantly groundwater-fed regimes, received 26% snowmelt runoff. Consequently, Martin River (lake-dominated) catchment had increased snowmelt contributions attributable to higher basin gradient and greater open area coverage. However, Martin River catchment exemplified a distinct hydrological regime that is not well represented in sampling surveys or monitoring networks, since enriched isotopic signatures at end-of-winter streamflow implied a lake water input rather than groundwater.

Important observations in isotopic composition of snow, particularly d -excess, and SWE reveal larger scale climate variability, such as the El Niño influence on annual temperatures in 1998, which initiated an earlier snowmelt response and extended the evaporative season. Information on atmospheric circulation obtained from snowpack is often impeded by depositional effects causing a loss in the air-mass source signature. Yet,

the interannual variability in d -excess and land cover distribution of snow may be systematic, and hence may provide an insightful way to understand the nature of air-mass circulation over varying temporal and spatial scales.

Overall, the timing and magnitude of source water components can be quantitatively determined through isotopic hydrograph separations by taking advantage of the seasonal variation of $\delta^{18}\text{O}$ and $\delta^2\text{H}$ source waters, and coupling this with detailed knowledge of the basin characteristics (i.e. role of subarctic wetlands on runoff response) the flow path of water can be inferred. Accordingly, a significant improvement in modelling accuracy may be achieved with the addition of isotope tracers to calibrate and validate current hydrological models (Stadnyk *et al.*, 2005). As a goal towards understanding water cycle processes, climate variability, and effects of anthropogenic alteration on water resources, stable isotopes in river discharge provide catchment-integrated information into hydrological processes over seasonal to decadal scales, allowing isotope tracer techniques to be advantageous in all areas of hydrological study.

ACKNOWLEDGEMENTS

This study was funded by grants from NSERC, the Mackenzie GEWEX Study, and the National Water Research Institute. We thank Tom Carter and Cuyler Onclin for graciously providing meteorological data and logistical and technical support. This paper benefited from the helpful suggestions of two anonymous reviewers.

REFERENCES

- Adams WP. 1981. Snow and ice on lakes. In *Handbook of Snow: Principles, Processes, Management and Use*, Gray DM, Male DH (eds). Pergamon Press: Toronto; 437–474.
- Aylsworth JM, Kettles IM. 2000. Distribution of peatlands. In *The Physical Environment of the Mackenzie Valley, Northwest Territories: A Base Line for the Assessment of Environmental Change*, Dyke LD, Brooks GR (eds). *Geological Survey of Canada Bulletin 547*. Geological Survey of Canada: Ottawa; 49–55.
- Aylsworth JM, Burgess MM, Desrochers DT, Duk-Rodkin A, Robertson T, Traynor JA. 2000. Surficial geology, subsurface materials, and thaw sensitivity of sediments. In *The Physical Environment of the Mackenzie Valley, Northwest Territories: A Base Line for the Assessment of Environmental Change*, Dyke LD, Brooks GR (eds). *Geological Survey of Canada Bulletin 547*. Geological Survey of Canada: Ottawa; 41–48.
- Cayan DR. 1996. Interannual climate variability and snowpack in the western United States. *Journal of Climate* **9**: 928–948.
- Cooper LW. 1998. Isotopic fractionations in snow cover. In *Isotope Tracers in Catchment Hydrology*, Kendall C, McDonnell JJ (eds). Elsevier Science: Amsterdam; 119–136.
- Coplen TB. 1996. New guidelines for reporting stable hydrogen, carbon, and oxygen isotope-ratio data. *Geochimica et Cosmochimica Acta* **60**: 3359–3360.
- Den Hartog G, Ferguson HL. 1978. Water balance-derived precipitation and evapotranspiration. In *Hydrological Atlas of Canada*, Fisheries and Environment Canada: Ottawa, Ontario; map.
- Dingman SL. 1973. Effects of permafrost on stream flow characteristics in the discontinuous permafrost zone of central Alaska. In *Proceedings of the Second International Conference on Permafrost*, National Academy of Sciences: Washington, DC; 447–453.
- Dyke LD. 2000. Climate of the Mackenzie river valley. In *The Physical Environment of the Mackenzie Valley, Northwest Territories: A Base Line for the Assessment of Environmental Change*, Dyke LD, Brooks GR (eds). *Geological Survey of Canada Bulletin 547*. Geological Survey of Canada: Ottawa; 21–30.
- Ecoregions Working Group. 1989. Ecoclimatic regions of Canada, first approximation. In *Ecoregions Working Group of the Canada Committee on ecological land classification, Ecological Land Classification Series 23*. Sustainable Development Branch, Canadian Wildlife Service, Environment Canada: Ottawa, Ontario.
- Edwards TWD, Wolfe BB, Gibson JJ, Hammarlund D. 2004. Use of water isotope tracers in high-latitude hydrology and paleohydrology. In *Long-Term Environmental Change in Arctic and Antarctic Lakes*, Pienitz R, Douglas MSV, Smol JP (eds). Kluwer Academic Publishers: Dordrecht, The Netherlands; 187–207.
- Environment Canada. 2002. Canadian climate normals 1971–2000. In *National Climate Archive; Climate Normals and Averages*, Environment Canada: Ottawa, http://www.climate.weatheroffice.ec.gc.ca/climate_normals/index_e.html [2 November 2004].
- Folland CK, Karl TR, Christy JR, Clarke RA, Gruza GV, Jouzel J, Mann ME, Oerlemans J, Salinger MJ, Wang S-W. 2001. Observed climate variability and change. In *Climate Change 2001: The Scientific Basis*, Houghton JT, Ding Y, Griggs DJ, Noguer M, van der Linden PJ, Dai X, Maskell K, Johnson CA (eds). Cambridge University Press: Cambridge; 99–181.
- Gat JR, Bowser CJ, Kendall C. 1994. The contribution of evaporation from the Great Lakes to the continental atmosphere: estimate based on stable isotope data. *Geophysical Research Letters* **21**: 557–560.

- Genereux DP. 1998. Quantifying uncertainty in tracer-based hydrograph separations. *Water Resources Research* **34**: 915–919.
- Gibson JJ, Edwards TWD. 2002. Regional water balance trends and evaporation–transpiration partitioning from a stable isotope survey of lakes in northern Canada. *Global Biogeochemical Cycles* **16**: DOI: 10-1029/2001GB001839.
- Gibson JJ, Prowse TD. 1999. Isotopic characteristics of ice cover in a large northern river basin. *Hydrological Processes* **13**: 2537–2548.
- Gibson JJ, Prowse TD. 2002. Stable isotopes in river ice: identifying primary over-winter streamflow signals and their hydrological significance. *Hydrological Processes* **16**: 873–890.
- Gibson JJ, Edwards TWD, Bursey GG, Prowse TD. 1993a. Estimating evaporation using stable isotopes; quantitative results and sensitivity analysis for two catchments in northern Canada. *Nordic Hydrology* **24**: 79–94.
- Gibson JJ, Edwards TWD, Prowse TD. 1993b. Runoff generation in a high boreal wetland in northern Canada. *Nordic Hydrology* **24**: 213–224.
- Gibson JJ, Prepas EE, McEachern PM. 2002. Quantitative comparison of lake throughflow, residency, and catchment runoff using stable isotopes; modelling and results from a regional survey of boreal lakes. *Journal of Hydrology* **262**: 128–144.
- Harris DM, McDonnell JJ, Rodhe A. 1995. Hydrograph separation using continuous open system isotope mixing. *Water Resources Research* **31**: 157–171.
- Hayashi M, Quinton WL, Pietroniro A, Gibson JJ. 2004. Hydrologic functions of wetlands in a discontinuous permafrost basin indicated by isotopic and chemical signatures. *Journal of Hydrology* **296**: 81–97.
- Hedstrom NR, Pomeroy JW. 1998. Measurements and modelling of snow interception in the boreal forest. *Hydrological Processes* **12**: 1611–1625.
- Heginbottom JA. 2000. Permafrost distribution and ground ice in surficial materials. In *The Physical Environment of the Mackenzie Valley, Northwest Territories: A Base Line for the Assessment of Environmental Change*, Dyke LD, Brooks GR (eds). Geological Survey of Canada Bulletin 547. Geological Survey of Canada: Ottawa; 31–39.
- Herrmann A, Lehrer M, Stichler W. 1981. Isotope input into runoff systems from melting snow covers. *Nordic Hydrology* **12**: 309–318.
- Kane DL, Stein J. 1983. Water movement into seasonally frozen soils. *Water Resources Research* **19**: 1547–1557.
- Laudon H, Seibert J, Kohler S, Bishop K. 2004. Hydrological flow paths during snowmelt: Congruence between hydrometric measurements and oxygen 18 in meltwater, soil water, and runoff. *Water Resources Research* **40**: DOI: 10-1029/2003WR002455.
- Lawrence JR, White JWC. 1991. The elusive climate signal in the isotopic composition of precipitation. In *Stable Isotope Geochemistry: A Tribute to Samuel Epstein*, Taylor Jr HP, O'Neil JR, Kaplan IR (eds). *Geochemical Society Special Publication No. 3*. Lancaster Press: San Antonio, TX; 169–185.
- Male DH, Gray DM. 1981. Snowcover ablation and runoff. In *Handbook of Snow, Principles, Processes, Management and Use*, Gray DM, Male DH (eds). Pergamon Press: Toronto; 360–435.
- Marsh P. 1990. Snow hydrology. In *Northern Hydrology: Canadian Perspectives*, Prowse TD, Ommanney CSL (eds). National Hydrology Research Institute, Environment Canada: Saskatoon, SK; 37–61.
- McNamara JP, Kane DL, Hinzman LD. 1998. An analysis of streamflow hydrology in the Kuparuk River Basin, Arctic Alaska: a nested watershed approach. *Journal of Hydrology* **206**: 39–57.
- Moser H, Stichler W. 1980. Environmental isotopes in ice and snow. In *Handbook of Environmental Isotope Geochemistry*, vol. 1, Fritz P, Fontes JCh (eds). Elsevier: New York; 141–178.
- National Wetlands Working Group. 1997. *The Canadian Wetland Classification System*, 2nd edition, Warner BG, Rubec CDA (eds). Wetlands Research Centre, University of Waterloo: Waterloo, Canada.
- Obradovic MM, Sklash MG. 1986. An isotopic and geochemical study of snowmelt runoff in a small arctic watershed. *Hydrological Processes* **1**: 15–30.
- Petrone RM, Griffis TJ, Rouse WR. 2000. Synoptic and surface climatology interactions in the central Canadian subarctic: normal and El Niño seasons. *Physical Geography* **21**: 368–383.
- Pietroniro A, Prowse TD, Hamlin L, Kouwen N, Soulis R. 1996. Application of a grouped response unit hydrological model to a northern wetland region. *Hydrological Processes* **10**: 1245–1261.
- Pomeroy JW, Gray DM, Shook KR, Toth B, Essery RLH, Pietroniro A, Hedstrom NR. 1998. An evaluation of snow accumulation and ablation processes for land surface modelling. *Hydrological Processes* **12**: 2339–2367.
- Price JS. 1987. The influence of wetland and mineral terrain types on snowmelt runoff in the subarctic. *Canadian Water Resources Journal* **12**: 43–52.
- Price JS, FitzGibbon JE. 1987. Groundwater storage–streamflow relations during winter in a subarctic wetland, Saskatchewan. *Canadian Journal of Earth Sciences* **24**: 2074–2081.
- Prowse TD. 1986. Ice jam characteristics, Liard–Mackenzie rivers confluence. *Canadian Journal of Civil Engineering* **13**: 653–665.
- Prowse TD. 1995. River ice processes. In *River Ice Jams*, Beltaos S (ed.). Water Resources Publications: Colorado; 29–70.
- Prowse TD, Conly FM, Church M, English MC. 2002. A review of hydroecological results of the Northern River Basins study, Canada. Part 1. Peace and Slave Rivers. *River Research and Applications* **18**: 429–446.
- Prowse TD, Marsh P. 1989. Thermal budget of river ice covers during breakup. *Canadian Journal of Civil Engineering* **16**: 62–71.
- Quinton WL, Roulet NT. 1998. Spring and summer runoff hydrology of a subarctic patterned wetland. *Arctic and Alpine Research* **30**: 285–294.
- Reedyk S, Woo MK, Prowse TD. 1995. Contribution of icing ablation to streamflow in a discontinuous permafrost area. *Canadian Journal of Earth Sciences* **32**: 13–20.
- Rennie JA, Reid DE, Henderson JD. 1981. Permafrost extent in the southern fringe of the discontinuous permafrost zone, Fort Simpson, N.W.T. In *Proceedings of the Third International Conference on Permafrost*. National Research Council of Canada: Ottawa, ON; 439–444.
- Rodhe A. 1987. *The origin of streamwater traced by oxygen-18*. PhD thesis, Uppsala University, Sweden.
- Rodhe A. 1998. Snowmelt-dominated systems. In *Isotope Tracers in Catchment Hydrology*, Kendall C, McDonnell JJ (eds). Elsevier Science: New York; 391–433.
- Rouse WR. 2000. Progress in hydrological research in the Mackenzie GEWEX study. *Hydrological Processes* **14**: 1667–1685.

- Schotterer U, Grosjean M, Stichler W, Ginot P, Kull C, Bonnaveira H, Francou B, Gaggeler HW, Gallaire R, Hoffmann G, Pouyaud B, Ramirez E, Schwikowski M, Taupin JD. 2003. Glaciers and climate in the Andes between the equator and 30 °S: what is recorded under extreme environmental conditions? *Climatic Change* **59**: 157–175.
- Stadnyk T, St Amour NA, Kouwen N, Edwards TWD, Pietroniro A, Gibson JJ. 2005. A groundwater separation study in boreal wetland terrain: The WATFLOOD hydrological model compared with stable isotope tracers. *Isotopes in Environmental and Health Studies* **41**: 49–60.
- Stewart RE, Leighton HG, Marsh P, Moore GWK, Ritchie H, Rouse WR, Soulis ED, Strong GS, Crawford RW, Kochtubajda B. 1998. The Mackenzie GEWEX Study: the water and energy cycles of a major North American river basin. *Bulletin of the American Meteorological Society* **79**: 2665–2684.
- Taylor S, Feng X, Kirchner JW, Osterhuber R, Klaue B, Renshaw CE. 2001. Isotopic evolution of a seasonal snowpack and its melt. *Water Resources Research* **37**: 759–769.
- Woo MK, diCenzo PD. 1989. Hydrology of small tributary streams in a subarctic wetland. *Canadian Journal of Earth Sciences* **26**: 1557–1566.
- Woo MK, Heron R. 1987. Effects of forests on wetland runoff during spring. In *Forest Hydrology and Watershed Management*, Swanson RH, Bernier PY, Woodard PD (eds). IAHS Publication No. 167. IAHS Press: Wallingford; 297–307.
- Woo MK, Winter TC. 1993. The role of permafrost and seasonal frost in the hydrology of northern wetlands in North America. *Journal of Hydrology* **141**: 5–31.
- Yang D, Woo MK. 1999. Representativeness of local snow data for large scale hydrologic investigations. *Hydrological Processes* **13**: 1977–1988.
- Zoltai SC, Tarnocai C, Mills GF, Veldhuis H. 1988. Wetlands of subarctic Canada. In *Wetlands in Canada*, National Wetlands Working Group (ed.). Ecological Land Classification Series 24. Environment Canada: Ottawa; 55–96.